

# Porous Euler-Lagrange Coupling: Application to Parachute Dynamics

Jason Wang<sup>1</sup>, Nicolas Aquelet<sup>1</sup>, Benjamin Tutt<sup>2</sup>  
Ian Do<sup>1</sup>, Hao Chen<sup>1</sup>, Mhamed Souli<sup>3</sup>

<sup>1</sup>*Livermore Software Technology Corporation  
7374 Las Positas Road, Livermore, CA 94550, USA  
aquelet@lstc.com*

<sup>2</sup>*Irvin Aerospace Inc.  
3701 West Warner Avenue, Santa Ana, CA 92704, USA  
Btutt@irvinaerospace.com*

<sup>3</sup>*Laboratoire de Mécanique de Lille UMR CNRS 8107  
Bd Paul Langevin – Cité Scientifique  
59655 Villeneuve d'Ascq cedex  
mhamed.souli@univ-lille1.fr*

## Abstract

*A newly developed approach for tridimensional fluid-structure interaction with a deformable thin porous media is presented under the framework of the LS-DYNA® software. The method presented couples a Arbitrary Lagrange Euler formulation for the fluid dynamics and a updated Lagrangian finite element formulation for the thin porous medium dynamics. The interaction between the fluid and porous medium are handled by a Euler-Lagrange coupling, for which the fluid and structure meshes are superimposed without matching. The coupling force is computed with an Ergun porous flow model. As test case, the method is applied to an anchored air parachute placed in an air stream*

## Introduction

Many important engineering applications such as airbags, parachute, to name a few, involve transient flows in deformable porous media [1]. In general the deformable porous media problem should be described at both the micro and macro scale. The problem at the microscopic level has a deformable skeleton surrounded by one or several fluids. At the macroscopic level the solid is usually described by the Lamé equations of linear elasticity and the fluid by the Navier-Stokes equations. The first simple model of a mechanical system comprised of a deformable porous solid matrix filled with a fluid has been developed by Biot [2] who formulated the macroscopic equations for the effective medium. The application of asymptotic homogenization methods [3,4] has lead to theoretical justification of Biot's equation [1,5,6] along with appropriate pore problems from which the macroscopic parameters can be computed numerically. The macroscopic equations are derived under the assumption that the solid-fluid interface displacements are small compared to the pore size. For a large class of poroelastic problems it is not possible to derive macroscopic equations. In general the upscaling problem for poroelasticity medium is not separable even when the pores are well separated. This is due to the fact that the

skeleton can deform arbitrarily large due to different parameters such as macroscopic displacements, pressure and velocity. However it is not practical to model the flow at the pore scale and undesirable to have to gather the tremendous amount of fine scale data that is required to model an entire parachute for example. Moreover present computational resources are not able to handle flow simulations of this size. Hence the models in this paper describe the essential physical behaviour in an averaged sense at the mega scale without modelling finer scale details. This assumption for thin porous media such as parachute seems reasonable. Actually the three phases that occur during a parachute mission are deployment, inflation, and terminal descent. The focus of this paper is the case when, due to problem parameters such as macroscopic pressure and velocity field for a parachute in inflation and terminal descent phases, the deformation of the fluid-solid interface is not considerable at the pore level. This interface could be approximated by a rigid motion of its initial position. Thus the porous coupling force is computed by using the Ergun equation [7] with a constant porosity. In this work, the governing equations for fluid and thin porous medium problem are first formulated together with boundary conditions. Then a description of the porous Euler-Lagrange coupling algorithm is presented. Further, this numerical method is applied to a porous parachute Fluid Structure Interaction problem by comparing the numerical results to experimental data.

### Fluid and Structure Modeling

The two applications described in this paper involve the modeling of a channel air flow interacting with a porous structure. The fluid is solved by using a Eulerian formulation [8] on a Cartesian grid that overlaps the porous structure, while this latter is discretised by Lagrangian shells based on the Belytschko-Lin-Tsay formulation [9].

In the applications the porous structures are nylon fabrics described at the macroscopic scale (\*MAT\_FABRIC). Let  $\Omega^s \in R^3$ , the domain occupied by the fabrics meshed by shell elements (\*ELEMENT\_SHELL) based on the Belytschko-Lin-Tsay shell formulation [9] (\*SECTION\_SHELL), and let  $\partial\Omega^s$  denote its boundary. An updated Lagrangian finite element formulation is considered: the movement of the thin porous medium  $\Omega^s$  described by  $x_i(t), (i=1,2,3)$  can be expressed in terms of the reference coordinates  $X_i(t), (i=1,2,3)$  and time  $t$ :

$$x_i = x_i(X_\alpha, t) \quad (1)$$

The momentum equation is given by Eq.(16) in which  $\bar{\sigma}$  is the Cauchy stress,  $\rho$  is the density,  $f$  is the force density,  $\frac{d\vec{v}}{dt}$  is acceleration and  $\vec{n}$  is the unit normal oriented outward at the boundary  $\partial\Omega^s$ :

$$\rho \frac{d\vec{v}}{dt} = \overline{\text{div}(\bar{\sigma})} + \vec{f} \quad (2)$$

$$\rho \frac{de}{dt} = \bar{\sigma} : \overline{\text{grad}(\vec{v})} + \vec{f} \cdot \vec{v} \quad (3)$$

The Lagrangian formulation for the fabric shells is input by the following keywords:

```

*PART
Canopy
$ pid, secid, mid
   1,      1,   1
*SECTION_SHELL
$ secid, elform
   1,      2
*MAT_FABRIC
$ mid,      ro      EA,   EB,   EC,   PRBA
   1, 533.77, 4.309e8,   0,   0,   0.14
*ELEMENT_SHELL
$ eid, pid, n1, n2, n3, n4

```

The solution of Eq.(2)-(3) satisfies the displacement boundary condition Eq.(4) on the boundary  $\partial\Omega_1^s$  and the traction boundary condition Eq.(5) on the boundary  $\partial\Omega_2^s$ .

$$\vec{x}(\vec{X}, t) = \vec{D}(t) \quad \text{on} \quad \partial\Omega_1^s \quad (4)$$

$$\vec{\sigma} \cdot \vec{n} = \vec{\tau}(t) \quad \text{on} \quad \partial\Omega_2^s \quad (5)$$

In the applications the traction boundary is the fluid-structure interaction surface. Thus the traction is the air pressure applied on the fabric canopy. In this paper the shell formulation used to model this canopy is the Belytschko-Lin-Tsay formulation [9]. The Belytschko-Lin-Tsay shell 4-node element is based on a co-rotational coordinate system and a constitutive computation using a rate of deformation. The embedded element coordinate system that deforms with the element is defined in term of four corner nodes. As the element deforms, an angle may exist between the fiber direction and the unit normal of the element coordinate system. The magnitude of this angle is limited in order to keep a plane shell geometry. In this local system, the Reissner-Mindlin theory gives the velocity of any point in the shell according to the velocity of mid-surface and the rotations of the element's fibers. Then, the rates of deformation are computed at the center of the element. The new Cauchy stresses are computed by using the material model and by accounting for the incremental rotation,  $\Delta\bar{R}$ . This latter is obtained by expressing the element base vectors at  $t(n+1)$  in the local system at  $t(n)$ . Since the material rotation is equal to the rotation of the local system,  $\Delta\bar{R}$  is the identity matrix. This involves the Belytschko-Lin-Tsay shell element is a computationally efficient alternative to the Hughes-Liu shell element. Then, the element-centered resultant forces and moments are obtained by integrating the stresses through the thickness of the shell. The relations between these forces and moments and the local nodal forces and moments are obtained by performing the principle of virtual power with one point quadrature. Finally, using the transformation relations defined by the global components of the corotational unit vectors derives the global nodal forces and moments. The following paragraph presents the description of the fluid.

Let  $\Omega^f \in R^3$ , represent the domain occupied by air defined by \*MAT\_NULL, and let  $\partial\Omega^f$  denote its boundary. This domain is meshed by solid elements (\*ELEMENT\_SOLID) based on a Eulerian formulation, which is a particular case of the ALE formulation (\*SECTION\_SOLID\_ALE). The equations of mass, momentum and energy conservation for the

air flow in a general ALE formulation in the reference domain, which is here the mesh are given by:

$$\frac{\partial \rho}{\partial t} + \rho \text{div}(\vec{v}) + (\vec{v} - \vec{w}) \cdot \text{grad}(\rho) = 0 \tag{6}$$

$$\rho \frac{\partial \vec{v}}{\partial t} + \rho (\vec{v} - \vec{w}) \cdot \overline{\overline{\text{grad}(\vec{v})}} = \overline{\overline{\text{div}(\sigma)}} + \vec{f} \tag{7}$$

$$\rho \frac{\partial e}{\partial t} + \rho (\vec{v} - \vec{w}) \cdot \overline{\overline{\text{grad}(e)}} = \overline{\overline{\sigma}} : \overline{\overline{\text{grad}(\vec{v})}} + \vec{f} \cdot \vec{v} \tag{8}$$

where  $\vec{f}$  is the body force and  $e$  is the specific internal energy.  $\vec{v}$  and  $\vec{w}$  are the fluid and mesh velocity fields respectively. If  $\vec{v} = \vec{w}$ , the equations (6)-(8) give the previous Lagrangian formulation. In the Eulerian formulation  $\vec{w} = \vec{0}$ , this assumption eliminates the remeshing and smoothing process, but does not simplify the Navier-Stokes equations (6)-(8). These equations are solved by the split approach detailed in [8],[10] and implemented in LS-DYNA®. In the equations (6)-(8)  $\rho$  is the density and  $\overline{\overline{\sigma}}$  is the total Cauchy stress given by:

$$\overline{\overline{\sigma}} = -p \cdot Id + \mu (\overline{\overline{\text{grad}(\vec{v})}} + \overline{\overline{\text{grad}(\vec{v})}}^T) \tag{9}$$

where  $p$  is the pressure and  $\mu$  is the dynamic viscosity. The pressure is computed by the ideal gas law (\*EOS\_IDEAL\_GAS):

$$p = \rho(Cp - Cv)T \tag{10}$$

where  $Cp$  and  $Cv$  are the specific heat capacities at constant pressure and volume respectively.

The Eulerian formulation is input by the following keywords:

```
*ALE_MULTI-MATERIAL_GROUP_PART
$ pid
  2
  3
*PART
Ambient air part
$ pid, secid, mid, eosid
  2,      2,    2,    2
*PART
Initial air part
$ pid, secid, mid, eosid
  3,      3,    2,    2
*SECTION_SOLID
$ secid, elform, aet
  2,      11    4
*SECTION_SOLID
$ secid, elform
  3,      11
*MAT_NULL
$ mid,    ro
```

```

2, 1.29
*EOS_IDEAL_GAS
$ eosid,      cv0,      cp0, c1, cq,      T0, V0
      2,      717.5, 1004.5,      0,  0, 270.1,  0
*ELEMENT_SOLID
$ eid, pid, n1, n2, n3, n4, n5, n6, n7, n8

```

The multi-material Eulerian formulation (\*ALE\_MULTI-MATERIAL\_GROUP\_PART and elform=11) is employed in order to highlight the effects of the porosity in the applications. Thus a part (pid=3) is created and the dummy material represents the initial air around the parachute. This initial material is pushed out of the Eulerian grid by the ambient material (pid=2), whose the solid elements occupy a layer at the inlet of the channel mesh.

Equations (6)-(8) are completed with appropriate boundary conditions. The part of the boundary at which the velocity is specified is denoted by  $\partial\Omega_1^f$ . The inflow boundary condition is:

$$\vec{v} = \vec{g}(t) \quad \text{on} \quad \partial\Omega_1^f \quad (12)$$

In the applications the channel flow is created by an inflow condition applied on the inlet nodes by the following keyword:

```

*BOUNDARY_PRESCRIBED_MOTION_NODE
$ nid, dof, vad, lcid

```

The traction boundary condition associated with Eq.(4) are the conditions on stress components. These conditions are imposed on the remaining part of the boundary of  $\Omega_1^f$ .

$$\vec{\sigma} \cdot \vec{n} = \vec{h}(t) \quad \text{on} \quad \partial\Omega_2^f \quad (13)$$

In the applications the traction boundary is the fluid-structure interaction surface ( $\partial\Omega_2^f = \partial\Omega_2^s$ ). Actually this boundary is the parachute and the traction force is computed by the porous coupling method implemented in the ALE formulation (\*CONSTRAINED\_LAGRANGE\_IN\_SOLID). The following section presents this method.

### Fluid – Porous Structure Interaction

In an explicit time integration problem the main part of the procedure in the time step is the calculation of the nodal forces. After computation of fluid and structure nodal forces we compute the forces due to the coupling, these will only affect nodes that are on the fluid - porous structure interface. For each structure node, a depth penetration  $\vec{d}$  is incrementally updated at each time step, using the relative velocity  $\vec{v}_{rel}$  at the slave and master node. For this coupling, the slave node is a structure mesh node, whereas the master node is not a fluid mesh node, it can be viewed as a fluid particle within a fluid element, with mass and velocity interpolated from the fluid element nodes using finite element shape functions. The location of the master node is also computed using the isoparametric coordinates of the fluid element. If  $\vec{d}^n$  represents the penetration depth at time  $t = t^n$ , it is incrementally updated in Eq.(14):

$$\vec{d}^{n+1} = \vec{d}^n + \vec{v}_{rel}^{n+1/2} \cdot \Delta t \quad (14)$$

In Eq.(14)  $\vec{v}_{rel}^{n+1/2} = \vec{v}_s^{n+1/2} - \vec{v}_f^{n+1/2}$  in which the fluid velocity  $\vec{v}_f$  is the velocity at the master node location and the structure velocity  $\vec{v}_s$  is the velocity at the slave node location. The coupling acts only if penetration occurs,  $\vec{n}_s \cdot \vec{d}^n < 0$ , where  $\vec{n}_s$  is built up by averaging normals of structure elements connected to the structure node. The porous coupling forces are derived from the integration of the Ergun Equation [7] on the shell volume:

$$\frac{dp}{d\hat{z}} = a(\mu, \varepsilon) \vec{v}_{rel} \cdot \vec{n}_s + b(\rho, \varepsilon) (\vec{v}_{rel} \cdot \vec{n}_s)^2 \quad (15)$$

in which  $\hat{z}$  is the local position along the fiber direction of the shell element and  $\varepsilon$  is the porosity. The coefficient  $a(\mu, \varepsilon)$  is the reciprocal permeability of the porous shell or viscous coefficient.  $b(\rho, \varepsilon)$  represents the inertia coefficient. For flows under very viscous conditions the second term in Eq.(15), which represents the inertia effects drops out and the Blake-Kozeny equation for laminar flows in porous media is obtained. At high rates of flow it is the first term or viscous term, which drops out and the Blurke-Plummer equation for turbulent flows in porous media is obtained. For the parachute application the inertia effects should be preponderant.

The force  $F$  derived from Eq.(15) is applied to both master and slave nodes in opposite directions to satisfy force equilibrium at the interface coupling, and thus the coupling is consistent with the fluid-structure interface condition namely the action-reaction principle. At the structure coupling node, we applied a force:

$$F_s = -F \quad (16)$$

whereas for the fluid, the porous coupling force is distributed to the fluid element nodes based on the shape functions, at each node  $i$  ( $i=1, \dots, 8$ ), the fluid force is scaled by the shape function  $N_i$ :

$$F_f^i = N_i \cdot F \quad (17)$$

Where  $N_i$  is the shape function at node  $i$ . Since  $\sum_{i=1}^8 F_f^i = F$ , the action-reaction principle is satisfied at the coupling interface.

In the applications the channel flow is created by an inflow condition applied on the inlet nodes by the following keyword:

```
*CONSTRAINED_LAGRANGE_IN_SOLID
$ slave, master, sstyp, mstyp, nquad, ctype, direc, mcoup
  145, 12, 0, 0, 2, 11
$ start, end, pfac, fric, frmin, norm, normtyp, damp
$ cq, hmin, hmax, ileak, pleak, lcidpor, nvent, iblock
$ iboxid, ipenchk, intforc, ialesof, lagmul, pfacmm, thk
  1
$ a1, b1, a2, b2, a3, b3
  1599174, 480514
```

The coupling with porous shells is defined by  $ctype=11$  and the one with porous solids corresponds to  $ctype=12$ . In this latter case all the coefficients on the last line can be defined for each directions (a1 and b1 for x-direction, a2 and b2 for y-direction and a3 and b3 for z-direction). For shells a1 and b1 are the viscous and inertia coefficients normal to the segment

respectively. The parameter *thk* is a scale factor of the shell thickness. The following paragraph presents the application of this approach to a porous disk parachute in terminal descent.

### Porous Parachute Application

A wind tunnel test of disk-gap-band parachute designs were carried out by Cruz and al. [11] in the framework of the Mars Exploration Rover mission. In this paper one of these parachutes named 1.6 Viking made in MIL-c-7020 type III fabric is modeled by the porous Euler-Lagrange coupling method. First the viscous and inertia coefficients must be determined by using the experimental permeability curve of the MIL-c-7020 type III fabric [12] (see Fig.1). Second the value of these parameters are checked with a model test. Finally the parachute model is performed.

### Determination of the Viscous and Inertia Parameters

As indicated in the introduction the porosity of the canopy is assumed constant. At the steady state the air density and dynamic viscosity are supposed uniform. Under these assumptions the viscous and inertia parameters in Eq.(15) are constant. The experimental permeability curve of the MIL-c-7020 type III fabric gives the rate of flow through the nylon canopy versus the pressure drop. To determine the viscous and inertia parameters in Eq.(15), the Ergun theoretical permeability should be a parabolical fit of the experimental one. Thus the coefficients *ax* and *bx* were computed by solving the following system:

$$\begin{cases} dp_1 / e = a.v_1 + b.v_1^2 \\ dp_2 / e = a.v_2 + b.v_2^2 \end{cases} \quad (18)$$

where  $e = 0.1016mm$  is the shell thickness and the couple of points  $(v_1, dp_1)$  and  $(v_2, dp_2)$  was chosen on the experimental plot so that the Ergun equation fits it as close as possible. The values of the viscous and inertia parameters are  $a = 1599174kg.m^{-2}.s^{-1}$  and  $b = 480514kg.m^{-3}$ .

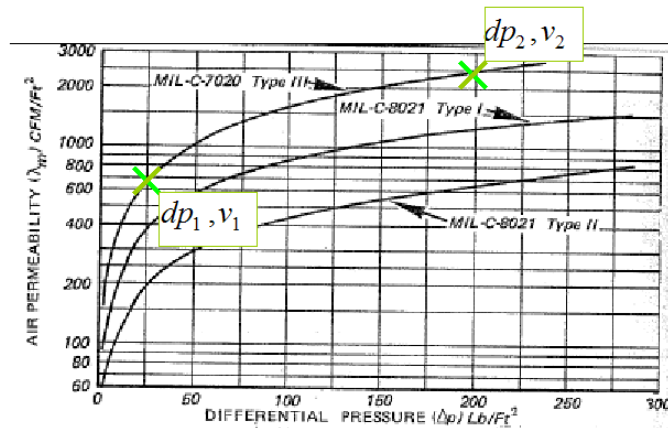


Figure.1 EXPERIMENTAL POROSITY CURVES [12]

A better approach to determine these coefficients should be to employ the following equations derived from the Ergun theory:

$$a = \frac{150\mu(1-\epsilon)^2}{D^2\epsilon^3} \quad (19)$$

$$b = \frac{1.75\rho(1-\varepsilon)}{D\varepsilon^3} \quad (20)$$

where  $\varepsilon$  is the porosity :  $\varepsilon = \frac{v_{void}}{v_{total}}$  and D is a characteristic length defined by:  $D = \frac{6(1-\varepsilon)V}{S}$

with V, the volume of the canopy and S, the “wetted” surface. However it is tricky to get the porosity of the MIL-c-7020 type III fabric in the literature.

The following application is dedicated to the validation of these parameters.

### Model Test

The model test is a channel with a constant prescribed rate of air flow at the inlet. The air density is  $1.29kg.m^{-3}$ . The channel sketched on Fig.2 is a Eulerian mesh of 3000 cubic solid elements based on the fluid formulation described previously. The first layer of solid elements on Fig.1 is composed of ambient or reservoir elements with a constant pressure. The square section of the channel is  $100m^2$ . A deformable nylon (MIL-c-7020 type III fabric,  $\rho = 533.77kg.m^{-3}$ ,  $E = 0.4309GPa$  ) shell occupies all one section of the channel, which is located at  $2m$  from the inlet. This membrane is meshed by 100 Lagrangian Belytschko-Lin-Tsay square shell elements. The simulation time is enough large to reach the steady state. It is  $20sec$ . The run takes about  $2h$  on a AMD Opteron Processor 248 (CPU: 2GHZ, cache size:1Mb) because of the time step is scaled down to avoid instability of the computation:  $\Delta t = 55\mu s$ . Actually the timestep needs to be adapted to prevent the run from crash. The higher the velocity is, the lighter the fabric is, the lower the time step should be.

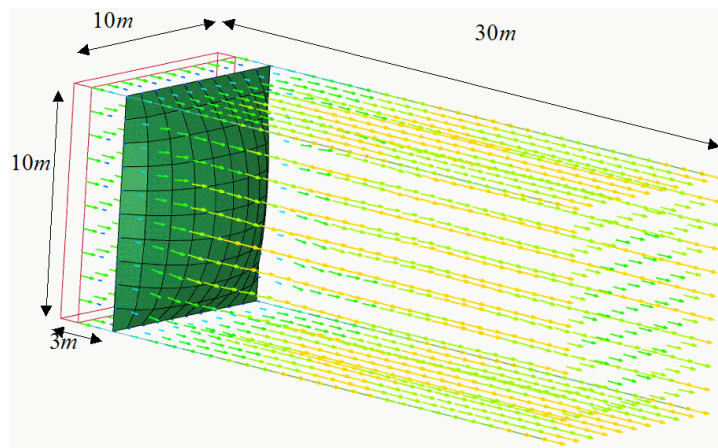


Figure 2. CHANNEL MODEL

The average pressure on the canopy at the steady state is post-treated for different inflow velocities. The purpose is to check if the porous behaviour of the fabric is well modeled. The rate of air flow through the deformed nylon shell enables to compute an average permeability velocity, for which the experimental and numerical pressure drops through the fabric are compared on Tab.1. :

Table 1. NUMERICAL AND EXPERIMENTAL PRESSURE DROPS

Inflow velocity ( <i>m/s</i> )	Permeability Velocity ( <i>m/s</i> )	Experimental Pressure Drop ( <i>Pa</i> )	Numerical Pressure Drop ( <i>Pa</i> )	Relative Errors (%)
10	2.7	862	794	9%
20	4	1628	1478	10%
30	5.4	2490	2316	7%
40	6.4	2969	3104	4%
50	7	3735	3653	2%

The slower the velocities are, the larger the relative errors on Tab.1 are. However the relative errors are acceptable. Thus the Ergun equation with  $a = 1599174 \text{kg.m}^{-2}.\text{s}^{-1}$  and  $b = 480514 \text{kg.m}^{-3}$  approximates well the porous behaviour of the MIL-c-7020 type III fabric which makes up the parachute canopy of the following paragraph.

### Parachute Model

The whole model is based on the informations of the article of Cruz et al. [11]. The geometry and dimensions of the released 1.6 Viking parachute and module models during the terminal descent are shown on Fig.3 .

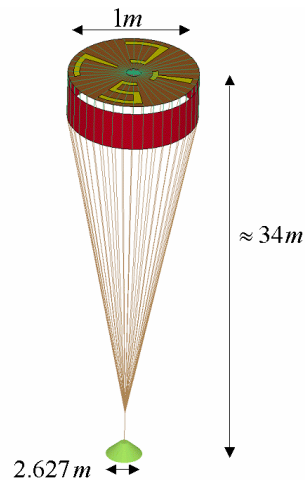


Figure 3. 1.6 VIKING PARACHUTE AND MODULE MODELS

The canopy and module walls are meshed by Lagrangian Belytschko-Lin-Tsay shells [9]. As for the model test air flow is modeled by an Eulerian mesh, which represents the wind tunnel. Thus the section of the Eulerian grid is a square of side  $4.8768\text{m}$  (16feet). The rate of flow is maintained by a constant velocity at the inlet for several Mach numbers: 0.134, 0.291 and 0.465. The air density is  $1.29 \text{kg.m}^{-3}$  and the sound speed is  $345 \text{m.s}^{-1}$ .

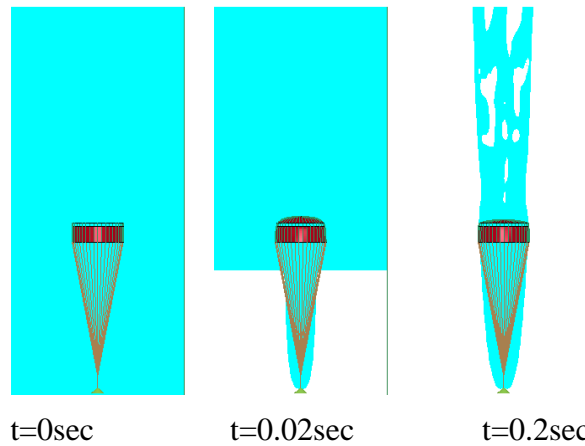


Figure 4. FLOW OF THE INITIAL AIR AT M=0.134

Figure 4 emphasizes the effect of the porous coupling on the air flow at M=0.134. On this figure the dynamics of the initial air is highlighted by a colored volume of fraction. A t=0sec air surrounding the parachute and filling all Eulerian domain has an initial velocity corresponding to the constant drop velocity of the module. Then this air is emptied out the computational fluid domain however a part is trapped in a vortex between the parachute and module. The trapped air can not only escape through the parachute vent but also through the porous canopy.

The drag force applied on the parachute canopy is investigated and the numerical drag coefficient at the steady state is compared to the experimental one given by [11]. The experimental drag coefficient is defined in [11] by Eq.(21):

$$C_D = \frac{F_D}{1/2\rho V^2 S_0} \tag{21}$$

where  $S_0$  is the nominal surface and  $V$  is the velocity at the inlet of the channel. The drag force  $F_D$  is a fluid-structure interaction force given by the database file, dbfsi.

For each Mach number the drag force oscillates more or less. These fluctuations are due to the wake of the backshell, which perturbs the steady state of the canopy. Thus the numerical drag force is gived on Tab.2 with an uncertainty like the experimental study. This range of force is defined by the highest and lowest values reached by the fluctuations.

Table 2. NUMERICAL AND EXPERIMENTAL DRAG COEFFICIENTS

Mach Number	Inflow Velocity (m/s)	Experimental Drag coefficient	Numerical Drag coefficient
0.134	46.23	0.44 ± 0.026	0.456 ± 0.02
0.291	100.39	0.457 ± 0.027	0.48 ± 0.08
0.465	160.42	0.477 ± 0.028	0.497 ± 0.048

On Tab.2 the experimental and numerical results are close. However the fluctuations make the estimation of the steady force tricky and they might affect the stability of the canopy. A

prospective investigation will model the stability of the parachute for which experimental data can be found in [11].

### Conclusion

This paper has described a method to solve fluid-structure interaction problem between a thin porous media and a fluid. This method was successfully applied to the porous problem of a disk parachute in terminal descent at constant velocity. The numerical and experimental results agree well. The prospective goal of this ongoing research will be to implement Ergun coefficients what will depend on the porosity, density and dynamic viscous.

### References

- [1] Bear, J., 1972, "Dynamics of fluids in porous media," Dover, New York.
- [2] Biot, M.A., 1941, "General theory of three dimensional consolidation," *J. Appl. Phys.*, **12**, pp.155–164.
- [3] Bensoussan, A., Lions, J.L., Papanicolaou, G., 1978, "Asymptotic analysis for periodic structures," *Studies in Mathematics and Its Applications*, **5**, North-Holland, Amsterdam.
- [4] Zhikov, V.V., Kozlov, S.M., Oleinik, O.A. 1994, "Homogenization of differential operators and integral functionals," Springer-Verlag, Berlin.
- [5] Sanchez-Palencia E., 1981, "Non-homogeneous media and vibration theory," *Lecture Notes in Physics*, **127**, Springer-Verlag, Berlin.
- [6] Mei, C.C., Auriault, J.-L., 1989, "Mechanics of heterogeneous porous media with several spatial scales," *Proc. Roy. Soc. Lond.*, **A 426**, pp.391–423.
- [7] Ergun, S., 1952, "Fluid flow through packed beds," *Chem. Eng. Prog.*, **48**(2), 89-94.
- [8] Benson D.J., 1992, "Computational methods in Lagrangian and Eulerian hydrocodes," *Computer Methods in Applied Mechanics and Engineering*, **99**(2), pp.235-394.
- [9] Belytschko T., Lin J., Tsay C.S., 1984, "Explicit algorithms for nonlinear dynamics of shells," *Comp. Meth. Appl. Mech. Engrg.*, **42**, pp-225-251.
- [10] Hughes, T.J.R., Liu, W.K., Zimmerman, T.K., 1981, "Lagrangian Eulerian finite element formulation for viscous flows," *J. Comput. Methods Appl. Mech. Engrg.*, **21**, pp.329-349.
- [11] Cruz, J. R., Mineck, R. E., Keller, D. F., Bobskill, M. V., "Wind Tunnel Testing of Various Disk-Gap-Band Parachutes," AIAA 2003-2129, 17th AIAA Aerodynamic Decelerator Systems Technology Conference and Seminar, 19–22 May 2003, Monterey, California.
- [12] Air Force Flight Dynamics Laboratory Technical Report (AFFDL-TR-78-151), Recovery Systems Design Guide, June 1978.

